Scientific Research Publishing

Mechanochemically Metamorphosed Composites of Homogeneous Nanoscale Silicon and Silicate Oxides with Lithium and Metal Compounds

Norihiro Shimoi[1*], Masae Komatsu[1], Yasumitsu Tanaka[2], Kazuyuki Tohji[1]

[1]Graduate School of Environmental Studies, Tohoku University, Sendai, Japan
[2]Institute for Excellence in Higher Education, Tohoku University, Sendai, Japan
Email: *norihiro.shimoi.c8@tohoku.ac.jp

Abstract

An active anode material for Li-ion batteries was synthesized using a simple mechanochemical process to minimize the large change in Si volume observed during charge-discharge operation and to compensate for the associated irreversible loss of Li or irreversible capacity loss, which are obstacles to achieve high-performance electrochemical properties during charge-discharge. The composite was mechanochemically milled with Si, lithium oxide, and copper oxide as raw materials; the composite contains Si nanoparticles, amorphous silicon monoxide, and Si-Li or Si-Cu alloy compounds, and it exhibits improved electrochemical properties. In particular, this composite achieved a better capacity retention, higher coulombic efficiency (over 100%), and longer cycling performance than Si alone, indicating considerable optimization of the electrical and ionic conductivity in the composite. The developed method allowed for control of the Li content to compensate for the lack of Li ions in the composite, and the cycling performance was optimized using the Cu alloy, oxide, and Li compounds within the composite.

Keywords

Mechanochemical Process, Nanocomposites, Metamorphosed Composites, Lithium-Ion Battery, Silicon Active Material

1. Introduction

Si-based Li-ion batteries (LIBs) have great potential because of the high capacity of the Si-based anodes relative to that of graphite anodes [1]. However, a major

obstacle to achieve a satisfactory reversible capacity in practical use is the large change in the Si volume observed during charge-discharge operations [2] [3] [4] [5] [6] and the irreversible formation of Li components. Many researchers have attempted to overcome these problems using nanostructures [4] [7]-[14] or other approaches, such as partial oxidization [7] [15] [16], composite formation with other materials [7] [9] [11] [17] [18] [19] [20], liquid-phase synthesis, and various battery production methods. Improvements in the stability of the prepared Si anodes have been observed from these attempts, leading to an improvement in LIB performance. We consider that further significant improvements may be obtained from synergistic effects when two or more approaches are simultaneously introduced in a simple operation. Accordingly, we reported the optimization of the cycling properties of an active Si anode by employing a composite of Si with CuO that was formed by a simple ball milling process with a planetary ball mill machine [21]. Here, we propose a mechanochemical approach that involves ball milling with Si, Li_2O, and CuO, and we describe the mechanism by which the obtained composite achieves a high charge-discharge performance. We successfully synthesized composites using homogeneous, nanoscale Si grains in a matrix of partially oxidized ground Si (SiO) as an active material. An LIB using the prepared composite showed a high initial coulombic efficiency (ratio between the reversible discharge capacity and the charge capacity) with good charge-discharge characteristics and an optimized cycling performance of over 3000 mAh/g after 800 cycles (Figure 1). The prepared composite of Si, Li_2O, and CuO shows improved electrical and ionic conductivities in the LIB system and is resistant to crystal collapse because of the expansion and contraction of Si in the composite. There are many reports of attempts to optimize both the electrical and ionic conductivities [22] [23] [24] [25] [26]; however, there are no previous attempts to synthesis active materials that include Li atoms to maintain the high performance of an LIB that lacks Li atoms for charge-discharge characteristics. We propose the synthesis of a composite with active Li compounds to compensate for the lack of Li ions in the anode of an LIB system along with Li-Si or other metal-Si alloys to optimize the electrical and ionic conductivities using a simple mechanochemical process.

2. Experimental

2.1. Composite of Si, Li_2O, and CuO Particles

A mixture of Si, Li_2O, and CuO particles (*i.e.* Si + Li_2O + CuO = 2.0 g) with average particle diameters of 4 μm (Kojundo Chemistry Laboratory Co., Ltd., Japan) was placed in a zirconia mill pot (45 cm^3 inner volume) with 7 zirconia balls (15 mm φ in diameter); ball milling was performed using a planetary ball mill machine (Fritsch Pulverisette-7) at approximately 600 rpm without heating and in air to produce aggregates composited with Si, Li_2O, and CuO. We then established a new anode composite to exploit the anticipated mechanochemical reaction between Si, Li_2O, and CuO when ground together. We designed particles
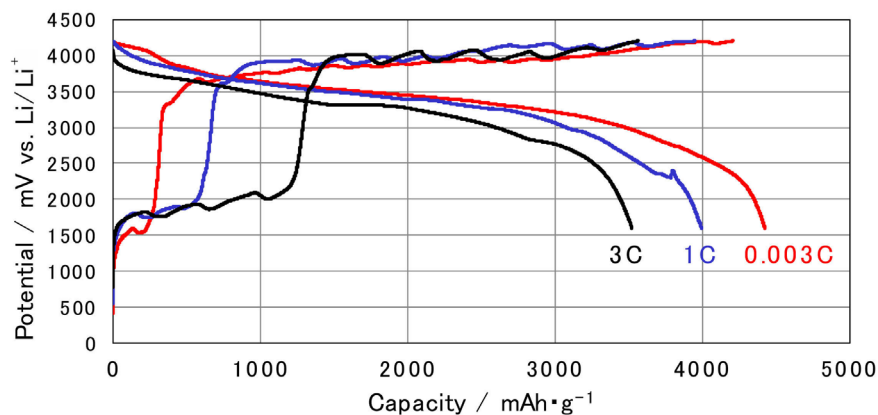
(a)
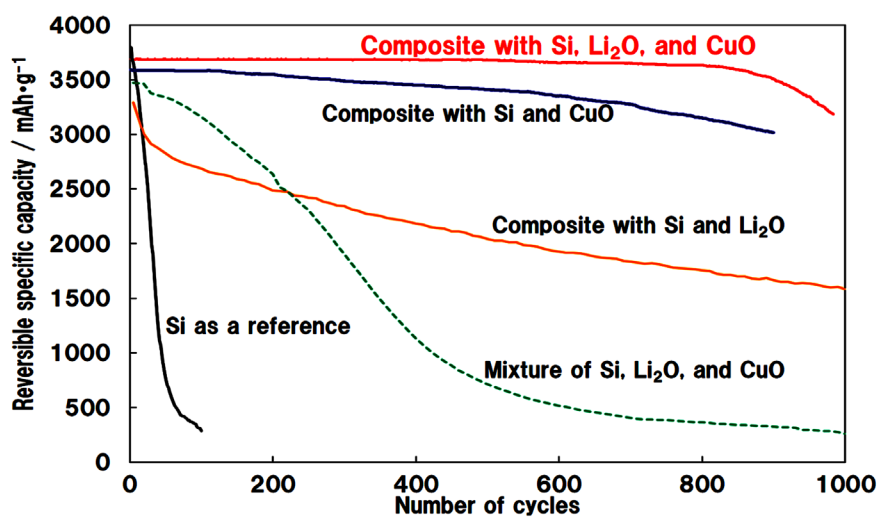
(b)

Figure 1. (a) Initial charge-discharge properties of the prepared composite with Si, Li$_2$O, and CuO at loading current densities of 0.01 mA/cm^2 (0.003 C), 3.2 mA/cm^2 (1 C), and 9.6 mA/cm^2 (3 C); (b) Comparison of the cycling properties of the anode with the prepared Si, Li$_2$O, and CuO composite (red line); Si and CuO composite (blue line); Si and Li$_2$O composite (green line); Si, Li$_2$O, and CuO mixture (dotted line); and Si particles as a reference (black line). The attenuation observed for the Si, Li$_2$O, and CuO composite after 800 cycles is due to peeling of the film from the Cu foil.

composited with Si (1.630 g), Li$_2$O (0.043 g), and CuO (0.327 g) for ball milling. The operation time for rotation of the ball mills was 3 h. Partial oxidation of Si at a molar ratio of Si:Li$_2$O:CuO of 10:0.25:0.75 endowed the composite with an excellent LIB performance.

2.2. Preparation of the Composite Electrodes

The Si composite electrodes were prepared as follows. The prepared composite was mixed with a binder composed of polyamic acid (Ube-kousan KK Company, Japan) and acetylene black (AB; Denkikagaku, Japan) as a conductive material in a 1-methyl-2-pyrrolidone solution. The Si composite:binder:AB weight ratio was 70:20:10. The slurry of the electrode components was cast onto a Cu

foil and dried at 70°C for 20 min in air. The cast electrodes were cut to 10 mm φ. The obtained electrodes had thicknesses in the range of 40 - 50 μm. The electrodes were further dried at 550°C under vacuum for 3 h and then pressed at 200 kgf/cm². The specific capacity was calculated according to the weight of the composite/binder/AB. Electrochemical tests of the composite electrodes were conducted using two-electrode test coin cells (type 2032; Housen, Japan) with a separator, and a gasket was used to hold the electrode in place.

2.3. Assembly of a Test Coin Cell for the LIB

The coin cells were assembled in an Ar-filled glove box using 1 M LiPF$_6$ in a mixed ethylene carbonate, diethylene carbonate, and dimethyl carbonate solution (60:25:15, v/v) as the electrolyte. For high charge-discharge operations, a LiCoO$_2$-coated film (300-μm thick) at a capacity of 12.0 mAh/cm² was employed as the cathode counter electrode, whereas a metal Li-foil was employed for impedance measurements. The separator was a polyethylene/polypropylene/polyethylene multi-stacked film with a thickness of 10 μm. The electrochemical performances of the two-electrode coin cells were evaluated using a potentiostat (Hokuto Denko Co. Ltd., Japan).

3. Results and Discussion

## 3.1. Electrochemical Properties of the Prepared Composite

Figure 1(a) shows the electrochemical performance of the composite anode evaluated in a 2032-type coin cell with a LiCoO$_2$ cathode in a constant-current charge-discharge test in the voltage range of 1.6 - 4.2 V with current densities of 0.01 mA/cm² (0.003 C), 3.2 mA/cm² (1 C), and 9.6 mA/cm² (3 C) at 27°C. The state of the charge of the battery was set to 100%. An LIB anode composed of Si, Li$_2$O, and CuO was fabricated on a Cu foil with a molar ratio of 10:0.25:0.75 to obtain good experimental charge-discharge characteristics. The results indicate that the charge and reversible discharge capacities depend on the components of the active material. The prepared composite, shown by the red line, exhibited an initial coulombic efficiency of 108.5% at a current density of 0.01 mA/cm² (0.003 C), as shown in Figure 1(a). The blue and black lines indicate that the initial coulombic efficiencies were 102.3% and 99.86% at current densities of 3.2 mA/cm² (1 C) and 9.6 mA/cm² (3 C), respectively. The average initial coulombic efficiency of the Si active material in the LIB was approximately 80%; however, the prepared composite attained a value of over 99% with a high loading rate. The Li compounds in the prepared composite may optimize the charge-discharge properties. We previously reported a mechanochemically synthesized composite of Si and CuO with a high initial coulombic efficiency of 95.1% [21]. The addition of Li ions is expected to improve the electrical and ionic conductivities of the active material. Moreover, because ceramic CuO and Li$_2$O are known as non-occlusive and non-conductive materials, respectively, they do not function as active materials in the LIB. In this study, the composites, which consist of ag-

gregates of Si, other conductive nanoscale grains, and a Si oxide material produced mechanochemically by ball milling, were successfully employed as anodes to occlude Li ions with a high coulombic efficiency from the first charge-discharge stage.

Figure 1(b) shows the cycling properties in the voltage range of 1.6 - 4.2 V at a current density of 9.6 mA/cm² (3 C) with $LiCoO_2$ employed as the cathode in a coin cell. The measured anodes employ a composite of Si, Li_2O, and CuO produced by a mechanochemical process (red line), a composite of Si and CuO (blue line), a composite with Si and Li_2O (yellow line), a mixture of Si, Li_2O, and CuO (dotted yellow line), and Si particles as a reference (black line). The Si/Li_2O/CuO and Si/CuO composites exhibited reversible capacities above 3000 mAh/g after 800 cycles; notably, the Si/Li_2O/CuO composite showed a high reversible capacity at 1000 cycles. This result contrasts with the behaviour of bare Si particles and the mixtures of Si/CuO and Si/Li_2O, which showed capacities below 50% after relatively few cycles. The Li_2O and CuO ceramics in the mixture do not function as active materials and have low cycling properties when mixed with Si, as shown in Figure 1(b). However, the Si/Li and Si/Cu compounds synthesized using the ball milling process with this mixture increase the electrical and ionic conductivities in the prepared composite, thereby helping to maintain a high capacity over 100 charge-discharge cycles.

3.2. Mechanochemical Composition

Mechanochemical processes have been widely studied [27] [28] [29]. One line of research has focused on mechanochemical reduction by employing one element and one compound [30] [31], such as the reduction of CuO by co-grinding with Al, Mg, or Si to form Cu powders [32]. However, the products obtained using equimolar CuO and Si fail to achieve high LIB performances because a Si oxide, probably SiO_2, synthesized by the mechanochemical process leads to excessive oxide atoms in Si, and the composite does not function as an active material. In contrast, at a molar ratio of 10:0.75, Si was partially oxidized by the oxide atoms in CuO, producing a composite with an excellent LIB performance. In this case, the chemical reaction between Si and CuO is given by Equation (1). Thus, we attempted to establish a new anode composite to exploit the anticipated mechanochemical reaction between Si and CuO upon ball milling.

$$3CuO + 4Si \rightarrow Cu_3Si + 3SiO \qquad (1)$$
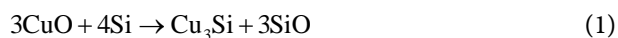
Furthermore, the mechanochemical reaction between Si and Li_2O when mixed at a molar ratio of 10:0.25 (Si:O) is expected to produce a composite by a non-equilibrium active reaction. Li has a lower electronegativity than Si or Cu formed by a mechanochemical process [32], does not react to reduce oxide atoms, and is not mechanochemically synthesized.

Figure 2 shows the crystallinity and ratio of components with Li atoms for the composite obtained by the mechanochemical process of Si, Li_2O, and CuO. The oxide atoms in CuO are reduced, and residual Cu is expected to form an alloy
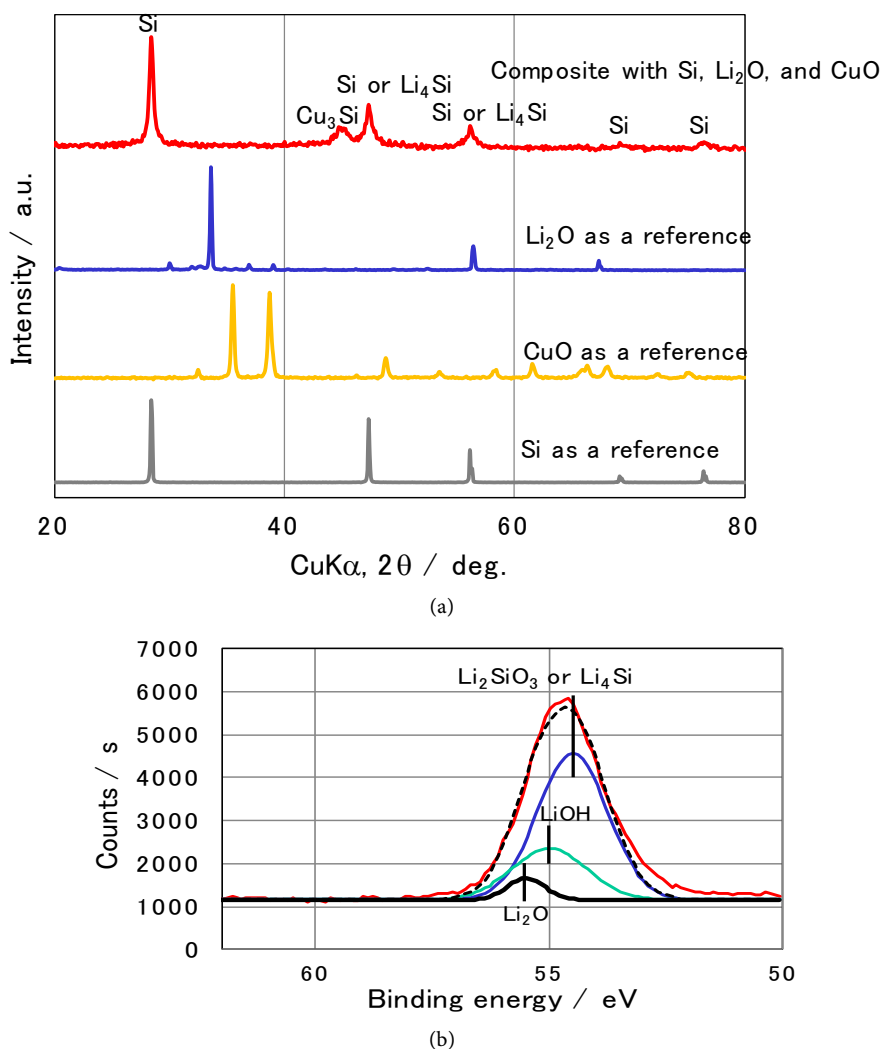
Figure 2. (a) XRD patterns of the Si, Li$_2$O, and CuO composite and each raw material before the ball milling process; (b) XPS spectrum of the prepared composite, enlarged in the region of the Li peak from 50 to 60 eV. The red spectrum can be deconvoluted into peaks corresponding to Li ions with various oxidation numbers. The Li ion peak mainly consists of Li$_2$SiO$_3$ or Li$_4$Si (blue line), with minor LiOH (aqua line) and Li$_2$O (black line) components.

with Si [27]. According to the X-ray diffraction (XRD; Rigaku Co. Ltd., Japan) pattern in **Figure 2(a)**, the Cu-Si alloy is in the form of Cu$_3$Si [33] and acts as a current collector; this alloy is electrically conductive and an important material for charge-discharge characteristics, which is determined by comparing the Si/Li$_2$O/CuO composite with the Si/Li$_2$O composite in **Figure 1(b)**, but does not function as an active material. In the XRD spectrum of the composite, no peaks are observed for CuO and Li$_2$O. Thus, the compounds synthesized from the reduction and oxidation of CuO or Li$_2$O were amorphous in the prepared composite. Si, Li, and the other oxide compounds were examined using high-resolution Si2p X-ray photoelectron spectroscopy (XPS; JEOL, Japan); a spectrum of the synthesized composite is shown in **Figure 2(b)**. A Si-Li oxide or Si-Li alloy is

expected to exist in the Si, Li$_2$O, and CuO composite. The enlargement of the XPS peak at ~50 - 60 eV, shown in **Figure 2(b)**, indicates the presence of a variety of Li ions with different oxidation numbers and mainly consists of Li-silicate oxide materials and Li alloys, namely Li$_2$SiO$_3$, Li$_4$Si, LiOH, and Li$_2$O. The content ratio of the different Li components in the composite was calculated by deconvolution of the peak position, which was calibrated using the C1s signal. Li was found mainly in the form of Li$_2$SiO$_3$ or Li$_4$Si throughout the synthesized composite, which confirms the presence of a Li-silicate oxide and Li-Si alloy in the composite, and the reaction outlined in Equation (2) is presumed. Moreover, CuO and Li$_2$O do not react with each other to form other components.

$$3Li_2O + 2Si \rightarrow Li_2SiO_3 + Li_4Si \tag{2}$$

Li$_2$SiO$_3$ has a higher free energy of formation than Li$_2$O and easily decomposes to a Si-Li oxide or Si-Li alloy; furthermore, Li$_2$SiO$_3$ does not function as an LIB active material.

Figure 3 shows an analysis of the prepared composite using scanning electron microscopy, scanning transmission electron microscopy, and transmission electron microscopy (SEM/STEM/TEM; Hitachi High-Technologies Co. Ltd.,
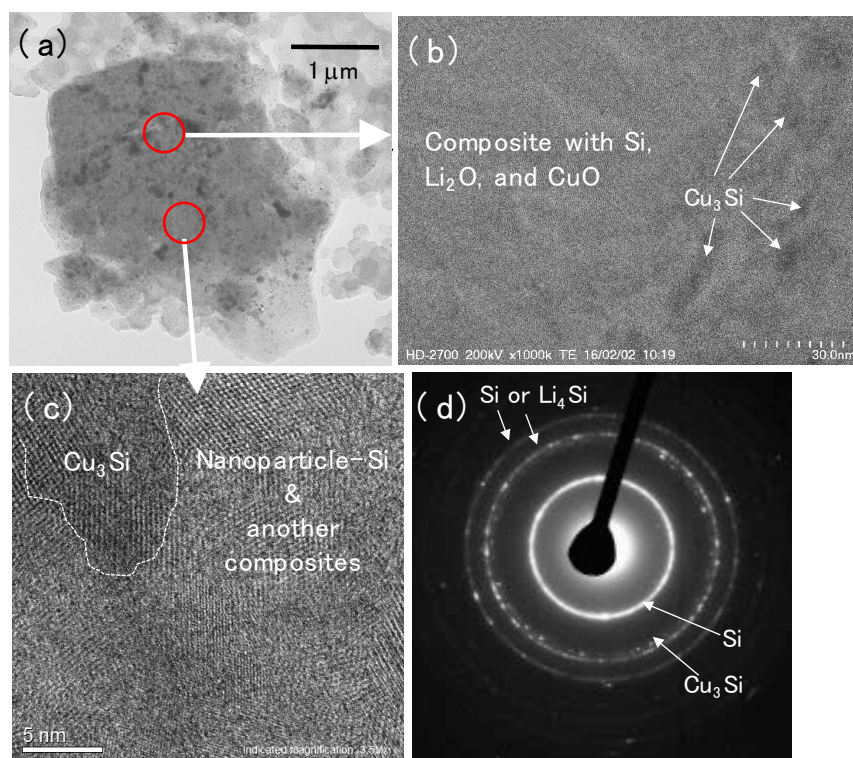

Figure 3. STEM images of the Si, Li$_2$O, and CuO composite. (a) SEM image showing the cross-sectional view of the microscale particles obtained by the ball milling process with Si, Li$_2$O, and CuO; (b) STEM cross-sectional view of the composite particle; (c) Enlarged STEM image of the areas marked in (a). The black area inside the white dotted line indicates Cu$_3$Si alloy grains in the composite particle; (d) TEM diffraction image showing the diffraction patterns of Si, Si-Li alloy, and Cu-Si alloy compounds in the STEM measurement area of (c).

Japan). The SEM overview image (**Figure 3(a)**) reveals the composite particles obtained by the ball milling process with Si, Li_2O, and CuO, and the STEM cross-sectional views in **Figure 3(b)** and **Figure 3(c)** show the bright field images of an anode electrode film in the areas indicated by red circles in **Figure 3(a)**. The bright grey areas in these images correspond to the composite of Si, Li, and O atoms, whereas the dark grey areas indicate the presence of Cu_3Si in the composite [21]. The crystal lattices indicate the orientation of each nanoscale Si or Li_4Si, and Cu_3Si crystal lattice from the results in **Figure 2(a)**. The high-resolution STEM images in **Figure 3(c)** confirm that each grain has a random crystal orientation and that the composite mainly comprises polycrystalline Si with nanoscale grains averaging 10 nm φ or Si-Li alloy grains, Cu_3Si nanoscale grains, and other compounds including a silicone monoxide and Li-silicate oxide components. **Figure 3(d)** represents crystallization of the prepared composite, nanoscale Si grains, and Cu_3Si grains.

The presence of Li or Cu in the composite is hypothesized to improve the electrical and ionic conductivities of the composite. Thus, impedance measurements were carried out to identify the elements that improve the electrical and ionic conductivities. **Figure 4** shows the impedance measurement results for the $Si/Li_2O/CuO$, Si/Li_2O, and Si/CuO composites, with that for Si particles as a reference. The samples were evaluated in a 2032-type coin cell with metal Li foil as the cathode. The $Si/Li_2O/CuO$ and Si/Li_2O composites, which include Li compounds, do not have a capacitance element in the impedance chart in **Figure 4(a)** in the low resistance range (shaded area), meaning that the ionic resistance element is almost zero when Li ions pass into the composite. Moreover, the impedance elements in **Figure 4(b)** in the high resistance range (shaded area) show that the composites including Li atoms have lower impedance elements, and the electrical conductance and ionic conductance are better than those of the other
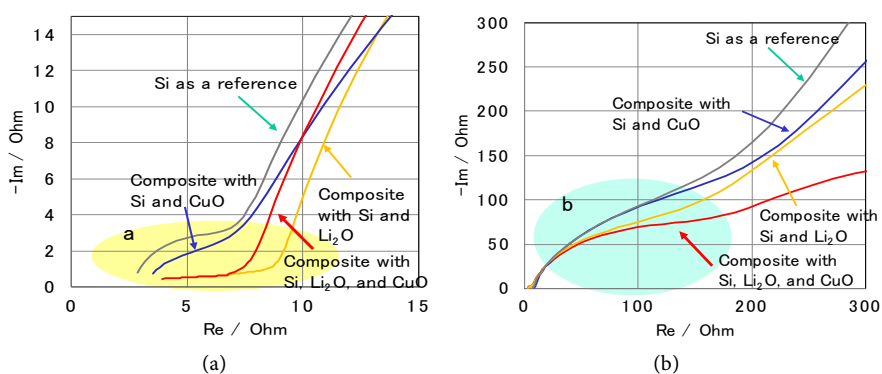

(a)

(b)

Figure 4. Comparison of the impedance charts of the composites with Si, Li_2O, and CuO (red line), Si and Li_2O (yellow line), and Si and CuO (blue line), with Si as a reference (green line). The shaded area of the impedance chart in (a) with a low resistance (<15 Ω) indicates the electrical and ionic conductivities of a Li ion passing into a particle and is modelled as a parallel circuit of capacitance and resistance. The shaded area of the chart in (b) with a high resistance (<300 Ω) indicates the impedance component passing through the border of a particle or from one particle to another.

composites that do not include Li atoms. These results confirm that the presence of Li compounds in the composite serve to improve the mobility of electrons and Li ions within the composite in LIBs.

3.3. Electrochemical Mechanism of the Composite

We observed punctate materials in the composite, leading us to surmise that the composite is a mixture of compounds of Si, Li_2O, and CuO. The atomic distributions of Si and Cu were determined using energy dispersive X-ray spectroscopy (EDX; Hitachi High-Technologies Corporation, Japan), and the reference Si atoms and Li atoms were detected using electron energy loss spectroscopy (EELS; Hitachi High-Technologies Corporation, Japan), as shown in Figure 5. Each distribution was measured before the initial charge and after 800 cycles. The EDX and EELS results show that the composite contained Si, Li, and Cu grains before the initial charge from the mechanochemical process. Si, Li, and Cu were homogeneously dispersed in the composite before the initial charge; after 800 cycles, Li atoms were practically non-existent in the composite. Li atoms in the composite could be used to discharge the capacity of the anode during charge-discharge operation to maintain a high capacity. In that case, an irreversible Li-Si alloy was synthesized during the charge-discharge process, and the synthesized Li atoms in the composite were made available to compensate for the capacity attenuation over many cycles. Moreover, a major obstacle to achieving a satisfactory reversible capacity in practical use lies in the large change in the Si volume observed during charge-discharge operation. The shape
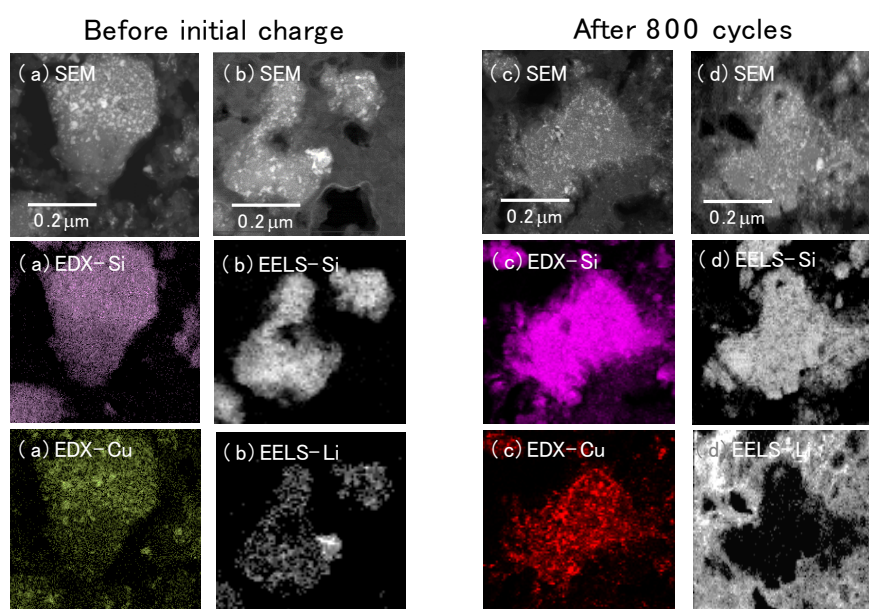

Figure 5. Distributions of Si and Cu by EDX and Si and Li by EELS in the composite with Si, Li_2O, and CuO. ((a) and (b)) SEM cross-sectional views of the composite with Si, Li_2O, and CuO before the initial charge, EDX distribution maps of Si and Cu, and EELS distribution maps of Si and Li. ((c) and (d)) SEM cross-sectional view of the composite with Si, Li_2O, and CuO; EDX and EELS maps after 800 charge-discharge cycles at 3000 mAh/g.

of the composite and atomic distributions of Si, Li, and Cu were maintained during the testing cycles, and no collapse of the structure was observed in the presence of SiO as a buffer matrix. The amorphous structure of SiO [34] [35] [36] [37] in the composite is expected to play a role in mitigating the expansion of active materials with nano-Si grains and including Li ions. In addition, **Figure 5(c)** and **Figure 5(d)** confirm that the composite did not change volume after the charge-discharge process, and crystal or nanoscale grain collapse was prevented during the expansion and contraction of Si in the prepared composite. In (d), EELS-Li revealed Li atoms distributed around the composite particle because Li atoms precipitated from the residual electrolyte in the LIB.

The specific gravity of the prepared composite is approximately 2.12 g/cm^3, which is less than the specific gravity of Si (2.33 g/cm^3). The prepared composite contains a matrix of silicon monoxide as a buffer material to maintain the expansion of the composite when inserting Li ions into Si nanoparticles and other active materials. This could prevent the expansion of Si and optimise the charge-discharge characteristics.

We expect a Li-Si alloy (likely Li$_4$Si) to be present in the composite; Li ion distribution in the prepared composite is demonstrated by the EDX measurements shown in **Figure 5**. Thus, the Si, Li$_2$O, and CuO composite is confirmed as an aggregate of nanoscale grains based on Si, Cu$_3$Si, and other materials. The structure of the composite is hypothesized in **Figure 6** to involve nanoscale Si grains to prevent cracking through numerous repetitions of the charge-discharge cycle [10] [13], Cu$_3$Si as a current collector, and amorphous SiO surrounding each Si grain to prevent cracking of Si.

We postulate that a composite material consisting of a poly-Si, Si oxide, Si-Cu alloy, Si-Li alloy, and Li-silicate oxide in a composite particle will likely
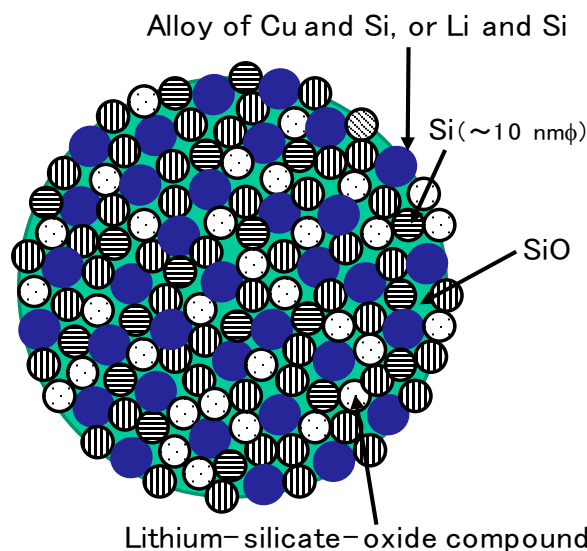

Figure 6. Structural image of the Si, Li$_2$O, and CuO composite as an aggregate of Si and Cu$_3$Si nanoscale grains on amorphous silicon monoxide with a Li-silicate oxide compound (likely Li$_2$SiO$_3$) and a Li-Si alloy (likely Li$_4$Si).

yield a good performance with respect to the charge-discharge characteristics in an LIB. The alloying of Li or Cu by mechanochemical processing can transform Si into a Si alloy or other oxide compound. Improvements in the stability of the Si anodes have been observed from such individual attempts, leading to improvements in the LIB performance [38] [39] [40]. We consider that further significant improvements will be obtained from synergistic effects when two or more approaches are simultaneously introduced in one simple operation.

4. Summary and Outlook

We produced a model for the high electrochemical performance of LIBs employing a Si, Li_2O, and CuO composite as an anode material. A high coulombic efficiency of over 100% and long cycling stability at a high loading current density of 3000 mAh/g were achieved, indicating that the composite acted as an active material with dispersed Si nanoscale grains or Li-Si compounds. Li-Si or Cu-Si alloys are expected to function electrochemically in the charge-discharge process. The Cu_3Si alloy in the prepared composite helps to improve the electrical conductivity; Li-Si compounds, which include Li_4Si and Li_2SiO_3, work to improve the electrical conductivity and compensate for the lack of Li ions in the composite during charge-discharge cycling. The diffusion of Li^+ into the composite that includes nano-Si grains, SiO, Li_2SiO_3, Cu_3Si, and Li_4Si in (a) of **Figure 7** results in an initial charge of the LIB, and an alloy of Li-Si or SiO is synthesized in the composite in (b), as well as an irreversible Si-Li alloy, which does not participate in the charge-discharge process. Furthermore, the Li ions remove SiO and some Li_4Si from nano-Si in (c), and the composited Li_4Si is transformed to $Li_{4-y}Si$. In (d), $Li_{4-y}Si$ receives Li atoms from Li_2SiO_3, which has a higher free energy of formation. The next charge occurs in (e). Li_2SiO_3 and Li_4Si in the composite may not be the actual compounds found in the composite because
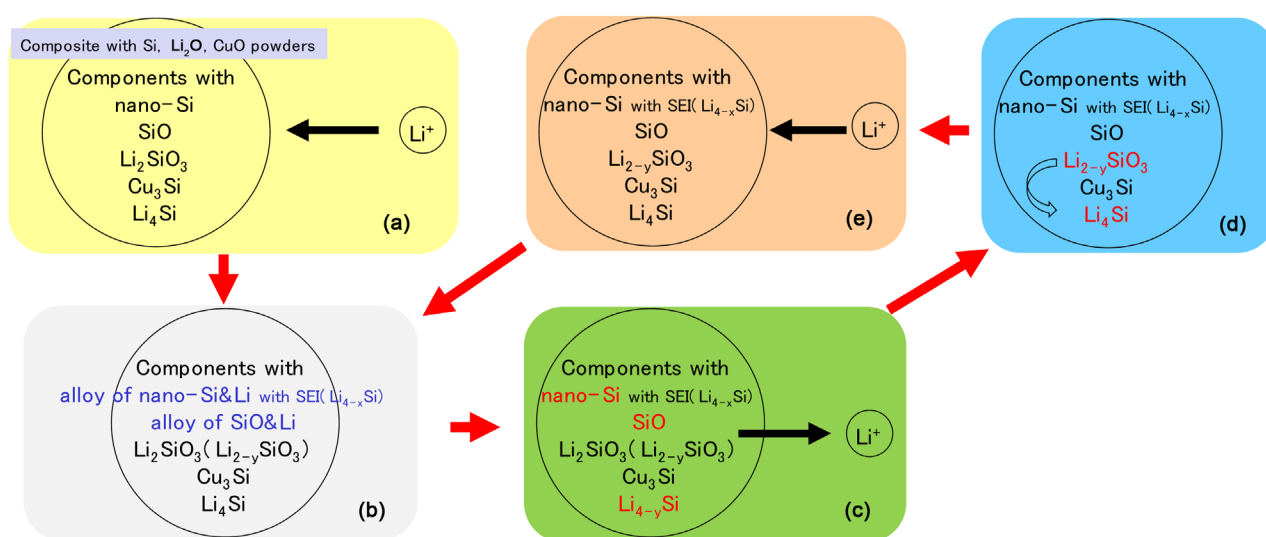

Figure 7. Model of a charge-discharge mechanism employing the composite with Si, Li_2O, and CuO to satisfy the high capacity and long cycling stability of the active anode material.

121

each material is assumed to be mixed as amorphous materials. Nonetheless, compounds in the composite that include Li atoms, such as Li_2SiO_3 and Li_4Si, are consumed before and after the charge-discharge process, and Li atoms are expected to be available to compensate for the lack of Li ions in the anode of the LIB.

We conclude that the structure of the composite unites the structural features of an active material based on a Si composite with a high capacity and cyclic reversible charge properties. The following observations were made:

1) A homogeneous dispersion of Cu_3Si nanoscale grains, Si nanoparticles, amorphous SiO, and Si-Li compounds was obtained using a simple mechanochemical process. The crystals of both Cu_3Si and Si nanoparticles align randomly when ground at 27°C in air.

2) Our prepared composite delivered a better capacity retention and coulombic efficiency (over 100%) than Si alone. The ground samples exhibited a better cycling ability than the simple mixtures, and we could show that the existence of a Si-Cu alloy, SiO, and Si-Li compounds in the composite are important factors for improving the cycling performance. Moreover, the electrochemical stability of Si with Cu_3Si, Li_2SiO_3, and Li_4Si synthesized by a ball milling process was important in controlling the cycling performance. We expect the controlled release of Li from the Li compounds formed in the composite to compensate for the lack of Li ions and Si oxide compounds in the composite and thus optimize the cycling performance.

Thus, we synthesized an active composite material to serve as an anode in an LIB using a simple mechanochemical process. Successful material preparation for a Si anode was performed with a smaller addition of CuO as a nonstoichiometric case, expanding our understanding toward mechanochemical processes. While optimizing our treating conditions for preparing the Si composite, we considered the different applications of nonstoichiometric reactions to other similar issues.

Acknowledgements

References

[1] Netz, A., Huggins, R.A. and Weppner, W. (2003) The Formation and Properties of Amorphous Silicon as Negative Electrode Reactant in Lithium Systems. *Journal of Power Sources*, **119-121**, 95-100. https://doi.org/10.1016/S0378-7753(03)00132-0

[2] Besenhard, J.O. (1999) Handbook of Battery Materials, Wiley-VCH, Weinheim.

[3] Huggins, R.A. (1989) Materials Science Principles Related to Alloys of Potential Use in Rechargeable Lithium Cells. *Journal of Power Sources*, **26**, 109-120. https://doi.org/10.1016/0378-7753(89)80020-5

[4] Obrovac, M.N. and Krause, L.J. (2007) Reversible Cycling of Crystalline Silicon Powder. *Journal of Electrochemical Society*, **154**, A103-A108.

https://doi.org/10.1149/1.2402112

[5] Liu, X.H., *et al.* (2012) Size-Dependent Fracture of Silicon Nanoparticles during Lithiation. *ACS Nano*, **6**, 1522-1531. https://doi.org/10.1021/nn204476h

[6] Zhao, K., *et al.* (2012) Concurrent Reaction and Plasticity during Initial Lithiation of Crystalline Silicon in Lithium-Ion Batteries. *Journal of Electrochemical Society*, **159**, A238-A243. https://doi.org/10.1149/2.020203jes

[7] Hu, Y.-S., *et al.* (2008) Superior Storage Performance of a Si@SiO$_x$/C Nanocomposite as Anode Material for Lithium-Ion Batteries. *Angewandte Chemie*, **47**, 1645-1649. https://doi.org/10.1002/anie.200704287

[8] Kovalenko, I., *et al.* (2011) A Major Constituent of Brown Algae for Use in High-Capacity Li-Ion Batteries. *Science*, **334**, 75-79. https://doi.org/10.1126/science.1209150

[9] Magasinski, A., *et al.* (2010) High-Performance Lithium-Ion Anodes Using a Hierarchical Bottom-Up Approach. *Nature Materials*, **9**, 353-358. https://doi.org/10.1038/nmat2725

[10] Szczech, J.R. and Jin, S. (2011) Nanostructured Silicon for High Capacity Lithium Battery Anodes. *Energy & Environmental Science*, **4**, 56-72. https://doi.org/10.1039/C0EE00281J

[11] Liu, N., *et al.* (2012) A Yolk-Shell Design for Stabilized and Scalable Li-Ion Battery Alloy Anodes. *Nano Letters*, **12**, 3315-3321. https://doi.org/10.1021/nl3014814

[12] Hu, L., *et al.* (2011) Si Nanoparticle-Decorated Si Nanowire Networks for Li-Ion Battery Anodes. *Chemical Communications*, **47**, 367-369. https://doi.org/10.1039/C0CC02078H

[13] Holzapfel, M., *et al.* (2006) Nano Silicon for Lithium-Ion Batteries. *Electrochimica Acta*, **52**, 973-978. https://doi.org/10.1016/j.electacta.2006.06.034

[14] McDowell, M.T., *et al.* (2012) Studying the Kinetics of Crystalline Silicon Nanoparticle Lithiation with *in Situ* Transmission Electron Microscopy. *Advanced Materials*, **24**, 6034-6041. https://doi.org/10.1002/adma.201202744

[15] Yang, J., *et al.* (2002) SiO$_x$-Based Anodes for Secondary Lithium Batteries. *Solid State Ionics*, **152-153**, 125-129. https://doi.org/10.1016/S0167-2738(02)00362-4

[16] Shimoi, N. and Tanaka, Y. (2012) Improvement in Si Active Material Particle Performance for Lithium-Ion Batteries by Surface Modification of an Inductivity Coupled Plasma-Chemical Vapor Deposition. *Electrochimica Acta*, **80**, 227-232. https://doi.org/10.1016/j.electacta.2012.07.006

[17] Hochgatterer, N.S., *et al.* (2008) Silicon/Graphite Composite Electrodes for High-Capacity Anodes: Influence of Binder Chemistry on Cycling Stability. *Electrochemical and Solid-State Letters*, **11**, A76-A80. https://doi.org/10.1149/1.2888173

[18] Jang, B.O., *et al.* (2013) Electrospun Co-Sn Alloy/Carbon Nanofibers Composite Anode for Lithium Ion Batteries. *Journal of Alloys and Compounds*, **574**, 335-340. https://doi.org/10.1016/j.jallcom.2013.05.063

[19] Wu, H., *et al.* (2012) Stable Cycling of Double-Walled Silicon Nanotube Battery Anodes through Solid-Electrolyte Interphase Control. *Nature Nanotechnology*, **7**, 309-315. https://doi.org/10.1038/nnano.2012.35

[20] Ebner, M., *et al.* (2013) Visualization and Quantification of Electrochemical and Mechanical Degradation in Li ion Batteries. *Science*, **342**, 716-720. https://doi.org/10.1126/science.1241882

[21] Shimoi, N., *et al.* (2015) Mechanochemical Approaches to Employ Silicon as a Lithium-Ion Battery Anode. *AIP Advances*, **5**, Article ID: 057142.

https://doi.org/10.1063/1.4921563

[22] Li, X., *et al.* (2015) Germanium Anode with Excellent Lithium Storage Performance in a Germanium/Lithium-Cobalt Oxide Lithium-Ion Battery. *ACS Nano*, **9**, 1858-1867. https://doi.org/10.1021/nn506760p

[23] Wang, K.-X., *et al.* (2015) Surface and Interface Engineering of Electrode Materials for Lithium-Ion Batteries. *Advanced Materials*, **27**, 527-545. https://doi.org/10.1002/adma.201402962

[24] Jung, S.C., *et al.* (2014) Sodium Ion Diffusion in Al_2O_3: A Distinct Perspective Compared with Lithium Ion Diffusion. *Nano Letters*, **14**, 6559-6563. https://doi.org/10.1021/nl503169v

[25] Li, J., *et al.* (2014) Artificial Solid Electrolyte Interphase to Address the Electrochemical Degradation of Silicon Electrodes. *ACS Applied Materials & Interfaces*, **6**, 10083-10088. https://doi.org/10.1021/am5009419

[26] Lee, D.J., *et al.* (2013) Nitrogen-Doped Carbon Coating for a High-Performance SiO Anode in Lithium-Ion Batteries. *Electrochemistry Communications*, **34**, 98-101. https://doi.org/10.1016/j.elecom.2013.05.029

[27] Suryanarayana, C. (2001) Mechanical Alloying and Milling. *Progress in Materials Science*, **46**, 1-184. https://doi.org/10.1016/S0079-6425(99)00010-9

[28] Tanaka, Y., Zhang, Q. and Saito, F. (2003) Mechanochemical Dechlorination of Trichlorobenzene on Oxide Surfaces. *The Journal of Physical Chemistry B*, **107**, 11091-11097. https://doi.org/10.1021/jp0276808

[29] Beyer, M.K. and Clausen-Schaumann, H. (2005) Mechanochemistry: The Mechanical Activation of Covalent Bonds. *Chemical Reviews*, **105**, 2921-2948. https://doi.org/10.1021/cr030697h

[30] Welham, N.J. (1998) Mechanochemical Reduction of $FeTiO_3$ by Si. *Journal of Alloys and Compounds*, **274**, 303-307. https://doi.org/10.1016/S0925-8388(98)00590-8

[31] Zhang, Q., *et al.* (2002) Sulphidization of Metal Oxides by Means of Mechanochemical Solid Reaction. *Chemistry Letters*, **31**, 1094-1095. https://doi.org/10.1246/cl.2002.1094

[32] Shengqi, X., *et al.* (1996) The Reduction of CuO by Si during Ball Milling. *Journal of Materials Science Letters*, **15**, 634-635. https://doi.org/10.1007/BF00579274

[33] Bernard, F., Souha, H. and Gaffet, E. (2000) Enhancement of Self-Sustaining Reaction Cu_3Si Phase Formation Starting from Mechanically Activated Powders. *Materials Science and Engineering: A*, **284**, 301-306. https://doi.org/10.1016/S0921-5093(00)00749-8

[34] Jolly, F., *et al.* (1999) Temperature Effects on the Si/SiO_2 Interface Defects and Suboxide Distribution. *Journal of Non-Crystalline Solids*, **245**, 217-223. https://doi.org/10.1016/S0022-3093(98)00864-3

[35] Nagao, Y., *et al.* (2004) Structural Analysis of Pure and Electrochemically Lithiated SiO Using Neutron Elastic Scattering. *Journal of the Electrochemical Society*, **151**, A1572-A1575. https://doi.org/10.1149/1.1787173

[36] Hohl, A., *et al.* (2003) An Interface Clusters Mixture Model for the Structure of Amorphous Silicon Monoxide (SiO). *Journal of Non-Crystalline Solids*, **320**, 255-280. https://doi.org/10.1016/S0022-3093(03)00031-0

[37] Mamiya, M., *et al.* (2001) Preparation of Fine Silicon Particles from Amorphous Silicon Monoxide by the Disproportionation Reaction. *Journal of Crystal Growth*, **229**, 457-461. https://doi.org/10.1016/S0022-0248(01)01202-7

[38] Hwa, Y., *et al.* (2013) Modified SiO as a High Performance Anode for Li-Ion Bat-

teries. *Journal of Power Sources*, **222**, 129-134.
https://doi.org/10.1016/j.jpowsour.2012.08.060

[39] He, M., *et al.* (2014) Monodisperse Antimony Nanocrystals for High-Rate Li-Ion and Na-Ion Battery Anodes: Nano versus Bulk. *Nano Letters*, **14**, 1255-1262.
https://doi.org/10.1021/nl404165c

[40] Larcher, D., *et al.* (2007) Recent Findings and Prospects in the Field of Pure Metals as Negative Electrodes for Li-Ion Batteries. *Journal of Materials Chemistry*, **17**, 3759-3772. https://doi.org/10.1039/b705421c